Sensitization Behavior of Gnaw Austenitic Stainless Steel Joints

Subodh Kumar
SantLongowal Institute of Engineering & Technology, (Deemed University), Longowal, Sangrur (Punjab), India-148106

A.S.Shahi
SantLongowal Institute of Engineering & Technology, (Deemed University), Longowal, Sangrur (Punjab), India-148106

ABSTRACT
The present work has been carried out to study the sensitization behavior of AISI 304L austenitic stainless steel weld, fabricated using GTAW (gas tungsten arc welding process). This weld was subjected to post weld thermal aging (PWTA) treatments lying in the sensitization range, viz. 700 ˚C for 30 minutes, 500 minutes and 1000 minutes for studying the influence of carbide precipitation on their metallurgical and corrosion properties. Microstructural studies of these weldments showed that all welds were essentially austenitic with the presence of a small amount of δ-ferrite. The microstructure of the welds was dendritic and δ-ferrite phase placed in interdendritic regions. The weld metal exhibits largely vermicular morphology of δ-ferrite, and when it was subjected to different PWTA treatments, carbide precipitation occurred along the δ-γ interface, the extent of which increases as the aging time increases. The heat affected zones (HAZ) of the welds, besides undergoing excessive grain coarsening during welding, played a significant role in contributing towards overall sensitization of these joints. Microhardness of the weldments (weld metal and HAZ) decreases as the aging time increases due to the reason that the matrix becomes depleted in solution strengtheners C and Cr, which contribute towards carbide precipitation. Corrosion studies conducted through measuring the degree of sensitization (DOS) of the weldments. It was found that the overall DOS of the joints increases as the post weld thermal aging time increases.

Keywords
AISI 304L SS; GTAW; sensitization; δ-ferrite; DOS.

1. INTRODUCTION
Stainless steels (SS) are widely used in a variety of industries and environments due to their good mechanical and corrosion properties [1]. Austenitic stainless steels (ASS) are a group of steels that contain nominally 18-25 wt.% chromium and 8-20 wt.% nickel. This group of stainless steels exhibits an attractive combination of high strength, good ductility, excellent corrosion resistance and a reasonable weldability. These properties make austenitic stainless steels as attractive candidate materials for use in a wide range of industries such as nuclear industry, petrochemical, chemical industry, biomedical, dairy industry, food industry etc. [1, 2].

Welding is one of the most widely used processes to fabricate austenitic stainless steel structures [3, 4], whereas intergranular corrosion due to sensitization is one of the most common problem encountered in austenitic stainless steel weldments during welding as well as in the service conditions. This is a well-known phenomenon called sensitization that occurs during welding, when these steels are subjected to a temperature range of 550˚C to 850˚C, chromium reacts with carbon and form chromium carbides and precipitate along the grain boundaries thus giving rise to adjacent regions that are depleted in chromium [5-7]. This sensitization phenomenon that occurs during welding becomes a cause of concern when these joints are further subjected to a temperature range less than 500˚C, as usually encountered in nuclear applications, where it is observed that the pre-existing carbides nuclei, that nucleate during welding, tend to grow during long exposure times [8, 9], which consequently affects their corrosion properties and hence service performance.

Since, sensitization being a problem associated with welding as well as post weld service conditions in the welded joints of austenitic stainless steels, the aim of present investigation was to study the sensitization behavior of the gas tungsten arc welded 304L austenitic stainless steel joints.

2. MATERIALS AND EXPERIMENTAL DETAILS
The base material used in the present study was in the form of AISI 304L austenitic stainless steel plates with dimensions of 200 mm x 100 mm x 6 mm, which are cut from a rolled sheet. The ER 308L austenitic stainless steel solid electrodes of 1.6 mm and 2.4 mm diameters were selected as the filler metal to fill the single V-groove butt-joint by GTAW process. The chemical compositions of the base and filler metals are presented in the Table 1.

Before welding, the plates were cleaned mechanically and chemically in order to remove any source of contaminations like rust, dust, oil, etc. One root pass and two main weld passes were carried out to fill the single V-groove with the experimental conditions mentioned in Table 2. The interpass temperature of around 150˚C was maintained for second and third passes. No preheat and post heat treatment was carried out on the welded samples. Welded joints were visually inspected (during and after the welding) for their quality and it was ensured that all weld beads possessed good geometrical consistency and were free from visible defects like surfaceporosity, blow holes etc. Industrial argon gas with 10 l/min was used for shielding the weld pool during welding.

Table 1: Chemical composition of the base and filler material (wt.%)

Alloy element	C	Si	Mn	P	S	Cr	Mo	Ni	Ti	V	Fe
Base (304L SS)	0.025	0.446	1.386	0.028	0.014	18.238	0.296	9.196	0.006	0.061	Balance
Filler (ER 308L SS)	0.028	0.421	1.420	0.021	0.012	19.151	0.256	10.02	0.003	0.032	Balance

Table 2: Experimental welding conditions used in the present work

Type of passes	Welding current (A)	Welding voltage (V)	Average welding speed (mm/s)	Heat input per unit length per weld pass (kJ/mm)
Root pass	90	10	1.48	0.43
Middle pass	140	14	1.32	1.04
Cover pass	140	14	1.27	1.08

In order to study the sensitization (carbide precipitation) behavior of these joints, three different post weld thermal aging treatments (CS) viz. 700˚C for 30 minutes, 700˚C for 500 minutes and 700˚C for 1000 minutes were used in the present work.

The cross-section of the test specimens were mounted and mechanically ground to 3000 mesh on SiC papers and finally polished on the cloth using a suspension of alumina powder. Electrolytic etching was used for revealing the microstructures of different zones of the weldments. 10 gms. of oxalic acid and 100 ml. of distilled water was used as the electrolyte using the etching conditions of 6V and 1 min. as cell voltage and etching time respectively. The microstructure of the different zones of the weldments like weld metal (WM), heat affected zone (HAZ) and fusion zone (FZ) was investigated by optical microscopy. A microhardness tester equipped with Vickers pyramid indenter was used for microhardness measurements along the longitudinal centerline of the welds. A 500 g load was applied on the indenter for 20s. A ferritescope (M30-Fischer) was used in the non-destructive evaluation to observe the ferrite content on the weldments in different regions.

The double loop electrochemical potentiokinetic reactivation test (DLEPR) was used to assess the sensitization behavior of the welded joint in accordance with the test conditions used in the previously reported studies [10-12]. As shown schematically in Fig. 1, the testing samples were cut out from the welded plate in such a way that the cross-sectional area of each specimen (which was taken as 15 x 6mm^2=90 mm^2) that was exposed directly to the test solution inDLEPR test. Before electrochemical test, all samples weremounted in the epoxy resin and then prepared metallographically by using emery paper up to 1000 grit. A solution of 0.5 M H_2SO_4 + 0.01 M KSCN was used for conducting DLEPR test.A standard cell was used to conduct the DLEPR tests with a reference electrode of saturated calomelelectrode (SCE), a graphite counter electrode, and a working electrode. The entire testing including determination of the polarization curves was carried out with the potentiostat(Make: Gamry Instruments, Model: Reference 600) which was controlled by the dedicated software. The entire DLEPR testing of the welded joints was carried out at room temperature and the electrochemical potential was varied from the open circuit potential to 300 mV (SCE) with a scan rate of 100 mV/min and then back to the open circuit potential at the same scan rate of 100 mV/min. The ratio of the reactivation current to the activation current multiplied by 100 was taken as a measure of the degree of sensitization (DOS). The reported values are an average of three tests for each sample.

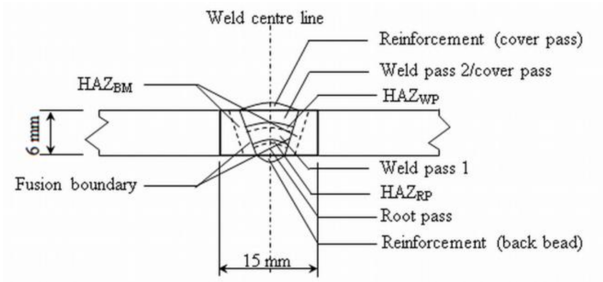

Fig. 1: Schematic illustration showing the cross-section of a welded joint and various zones formed in this joint.(Rectangular box at the centre shows the composite zone selected from the joint for DLEPR test).

3. RESULTS AND DISCUSSION

Ferrite studies were carried out to check the susceptibility of the weld metal to hot-fissuring tendency and it was found thatthe weld metal contains 5.1 to 5.8 % of the ferrite, which shows that this weld was not prone to hot cracking tendency. Few micrographs of the weld metal in the as welded and different post weld thermal aging conditions are shown in Fig. 2. The microstructure of the weld metal is dendritic, in which δ-ferrite phase placed in the interdendritic regions. The microstructure of weld metal possesses vermicular ferrite morphology. Fig. 2 shows that the carbide precipitation takesplace along the δ-γ interface [13] and this precipitation increases as the post weld thermal aging time increases. Fig. 3 shows the HAZ microstructures in the as welded and different post weld thermal aging conditions. From this Fig. 3, it is observed that HAZ experiences grain coarsening during welding, which may be attributed to the cooling rate experienced by the weld. This grain coarsening further affects the carbide precipitation behavior of the HAZ of the welded joint. From Fig. 3, it can be seen that as the post weld thermal aging time increases the carbide precipitation in the HAZ also increases.

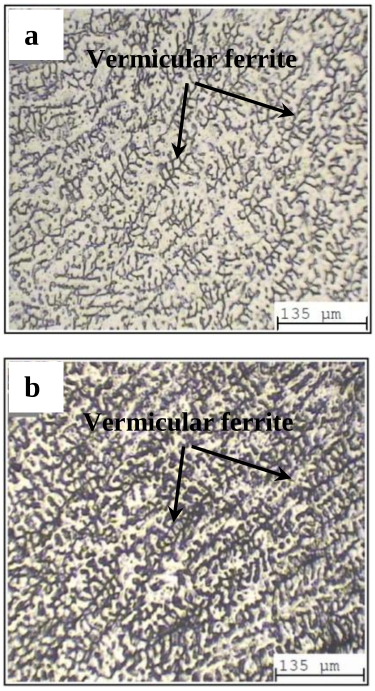

Fig. 2: Microstructure of the weld metal (at 100X) (a) as-welded and (b) PWTA (700˚C/1000 minutes) conditions.

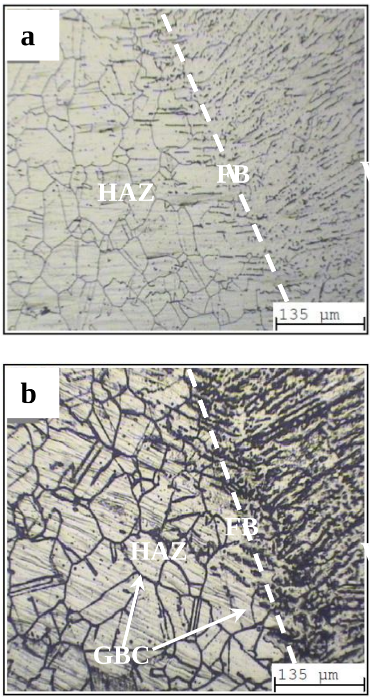

Fig. 3: Microstructure of the HAZ (at 100X) (a) as-welded and (b) PWTA (700˚C/1000 minutes) conditions.

Different zones of the weldments (as welded and post weld thermally aged) were evaluated for their microhardness and the results (which have average of five microhardness values for various zones of the each joint) are shown in the Table 3. It has been observed that among all the conditions, the weld zones possess relatively higher average microhardness value as compared to the respective HAZs, which may be attributed to the microstructural variations that occur in these zones during welding. It can also seen that average microhardness of the weld zones and the HAZs (for all the post weld thermally aged joints) show a decreasing trend due to the reason that the matrix becomes depleted in solution strengtheners C and Cr, which contribute towards intergranular carbide precipitation [14], and this precipitation increases with increased exposure times. Further, the extent of microhardness variation between the as welded condition and the post weld thermally aging at 700 ˚C for 1000 minuteswas such that average microhardness of the weld zone and HAZfor the joint, decreased from 221.52 to 201.23 VHN in the weld zone and 211.18 to 185.67 VHN in the HAZ, which may be attributed to higher carbide precipitation.

Table 3: Vickermicrohardness ($HV_{0.5}$) of the WM, HAZ and base metal under different conditions

S. No.		Vickermicrohardness ($HV_{0.5}$)			
		As-welded condition	Post weld thermal aging treatment at 700˚C		
			30 minutes	500 minutes	1000 minutes
1.	WM	221.52	219.13	210.74	201.23
2.	HAZ	211.18	209.54	195.25	185.67
3.	Base	225.33	223.12	208.41	198.74

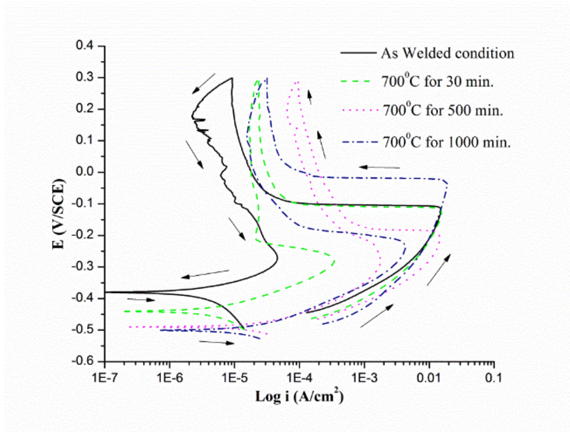

Fig 3: DLEPR curves of the welded joint under various conditions.

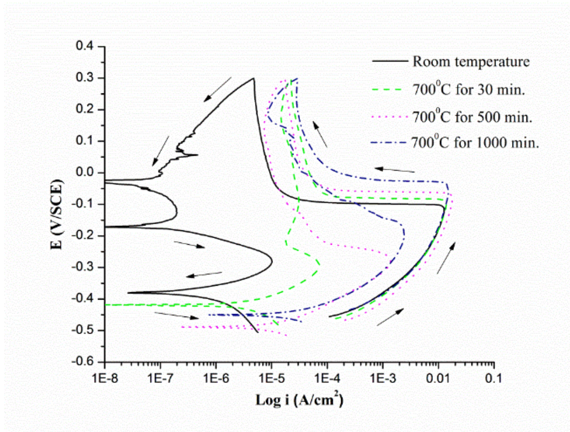

Fig 4: DLEPR curves of the base metal under various conditions.

Table 4: DLEPR results (DOS values of base metal and welded joints under different conditions)

S. No.		Degree of sensitization (DOS=(Ir/Ia)*100)			
		As-welded condition	Post weld thermal aging treatment at 700˚C		
			30 minutes	500 minutes	1000 minutes
1.	Welded joint	0.31	2.23	12.21	22.61
2.	Base	0.078	0.53	7.78	16.11

DLEPR technique was used for evaluating DOS of the welded joints andbase metal under different post weld thermal aging conditions, and the DLEPR curves are shown in the Fig. 3 &4 respectively. Table 4 shows the DLEPR results andfrom this table it can be seen that in the as welded condition, the welded joint possesses 0.31, DOS value and when this joint was subjected to post weld thermal aging treatments, the DOS value shows an increasing trend of varying degree.Maximum DOS (22.61) was observed for the weldedjoint subjected to 700˚C for 1000 minutes. This significant DOS variation is attributable to the mechanism involved for carbideprecipitation in the weld metal andHAZ of these welded joints, where, as the post weld thermal aging time increases the carbide precipitation (which occurs along δ-γ interfaces in the weld metal and along the grain boundaries in the HAZ) is also increases [15-16].

4. CONCLUSIONS

1. The weld metal matrix was austeniticwith the presence of a small amount of δ-ferrite and the morphology of the δ-ferrite was vermicular. When this weld metal was subjected to different PWTA treatments, carbide precipitation occurred along the δ-γ interface and the extent of this precipitation increases as the aging time increases.

2. HAZ of the welded joint experiences grain-coarsening during welding. When the welded joint subjected to various PWTA treatments, carbide precipitation occurred along the grain boundaries of the HAZ and the amount of this carbide precipitation increases as the aging time increases.

3. Microhardness evaluation of the welded joint showed that after PWTA treatments, the microhardness value of the base metal, weld metal and HAZ show a decreasing trend, which may be due to that the intense carbide precipitation removes chromium and carbon from solid solution.

4. DLEPR curves of the welded joint showed that as the post weld thermal aging time increases, the DOS value of the welded joint also increases.

5. REFERENCES

[1] Khatak, H. S. and Raj, B., 2002. Corrosion of Austenitic Stainless Steels. Narosa Publishing House, India.

[2] Sedrics, A. J., 1996. Corrosion of Stainless Steels. second ed., John Wiley & Sons, New York.

[3] Liu, W., Wang, R.J., Han, J.L., Xu, X.Y., Li, Q., 2010. Microstructure and mechanical performance of resistance spot welded cold-rolled high strength austenitic stainless steel. Journal of Materials Processing Technology, 210, 1956-1961.

[4] Zumelzu, E., Sepulveda, J., Ibarra, M., 1999. Influence of microstructure on the mechanical behavior of welded316L SS joints. Journal of Materials Processing and Technology, 94, 36-40.

[5] Ozyurek, D., 2008. An effect of weld current and weld atmosphere on the resistance spot weldability of 304L austenitic stainless steel. Materials and Design, 29, 597-603.

[6] Bruemmer, S.M. andCharlot, L.A., 1986. Development of grain boundary chromium depletion in type 304 and 316 stainless steels. ScriptaMetallurgica, 20, 1019-1024.

[7] Parvathavarthini, N., Dayal, R. K., Gnanamoorthy, J. B., 1994. Influence of prior deformation on the sensitization of AISI Type 316LN stainless steel. Journal of Nuclear Materials, 208, 251-258.

[8] Povich, M.J., 1978. Low temperature sensitization of type 304 stainless steel. Corrosion, 34, 60-65.

[9] Kain, V., Chandra, K., Adhe, K.N., De, P.K., 2004. Effect of cold work on low-temperature sensitization behaviourof austenitic stainless steels. Journal of Nuclear Materials, 334, 115-132.

[10] Lopez, N., Cid, M., Puiggali, M., Azkarate, I., Pelayo, A., 1997. Application of double loop electrochemical potentiodynamic reactivation test to austenitic and duplex stainless steels. Materials Science and Engineering A, 229, 123-128.

[11] Cihal, V. andStefec, R., 2001. On the development of the electrochemical potentiokinetic method. ElectrochimicaActa, 46, 3867–3877.

[12] Gracia, C., Tiedra de, M.P., Blanco, Y., Martin, O., Martin, F., 2008. Intergranular corrosion of welded joints of austenitic stainless steels studied by using an electrochemical minicell. Corrosion Science, 50, 2390-2397.

[13] Dadfar, M., Fathi, M.H., Karimzadeh, F., Dadfar, M.R., Saatchi, A., 2007. Effect of TIG welding on corrosion behaviour of 316L stainless steel. Materials Letters, 61, 2343-2346.

[14] Yae Kina, A., Souza, V.M., Tavares, S.S.M., Pardal, J.M., Souza, J.A., 2008. Microstructure and intergranular corrosion resistance evaluation of AISI 304 steel for high temperature service. Materials Characterization, 59, 651-655.

[15] Cui, Y. andLunding, C.D., 2005. Evaluation of initial corrosion location in E316 austenitic stainless steel weld metals. Materials letters, 59, 1542-1546.

[16] Cui, Y. andLunding, C.D., 2007. Austenite-preferential corrosion attack in 316 austenitic stainless steel weld metals. Materials and Design, 28, 324-32